Theor Chem Acc (2003) 110: 322–327
DOI 10.1007/s00214-003-0480-0

Theoretical
Chemistry Accounts

Regular article

Ab initio and density functional studies on the structure and vibrational spectra of 2-hydroxy-1,4-naphthoquinone-1-oxime derivatives

Kaustubh A. Joshi[1], **Dilip R. Thube**[2], **Sandhya Y. Rane**[1], **Shridhar P. Gejji**[1]

[1] Department of Chemistry, University of Pune, 411 007, Pune , India
[2] Department of Chemistry, New Arts, Commerce and Science College, Parner, Dist-Ahmednagar 414302, India

Received: 6 May 2003 / Accepted: 17 June 2003 /

Abstract. Structure and vibrational frequencies of lawsoneoxime and its C_3-substituted ($R = CH_3$, NH_2, Cl, NO_2) derivatives in keto and nitrosophenol forms have been obtained employing the Hartree–Fock and density functional methods. Charge distributions in different conformers have been studied using the molecular electrostatic potential topography as a tool. For all these derivatives except for nitrolawsoneoxime the amphi conformer in the keto form is predicted to be of lowest energy, which can partly be attributed to hydrogen bonding through the oximino nitrogen. In the nitro derivative, however, the preference to form a six membered ring owing to O–H–O hydrogen-bonded interactions makes the anti conformer (keto) the stablest. Further one of the nitrosophenol conformers of nitrolawsoneoxime turns out to be very close in energy (0.21 kJ mol^{-1} higher) to this anti conformer. The consequences of hydrogen bonding on charge distribution and vibrational spectra are discussed.

Keywords: Hartree–Fock – Density functional – Hydrogen bonding – Lawsoneoxime

Introduction

Lawsoneoxime and its C_3-substituted derivatives form an important class of ligands [1, 2, 3] since the quinone framework and the oxime group at the C_1 position result in enhanced donor capacity through O–O as well as O–N linkages, which facilitates their use in biomimics of self-organized molecular assemblies in photosystem II, wherein water oxidizes to molecular oxygen [4, 5, 6, 7, 8]. These ligands exist in fully oxidized quinone, semiquinone as well as fully reduced catecholate forms [3]. In particular the oxime derivatives of quinone-based ligands, for example, lawsone monoxime and related systems, stabilize the higher oxidation states of the metal ions, which leads to interesting magnetic and catalytic behaviour [9, 10, 11, 12]. Stereoisomers of lawsone monoxime and the derivatives along with nitrosophenol tautomers have been predicted from NMR experiments [13] and it has been inferred that the relative abundance of syn and amphi stereoisomers is governed by steric as well as hydrogen-bonding interactions. Although the structure of 3-methyl-2-hydroxy-1,4-naphthoquinone-1-oxime has recently been established [14] the molecular structures of this class of ligands have not yet been reported. Thus in order to gain deeper understanding of the binding of these ligands with metal ions we derive the structure, energies, charge distribution and the vibrational spectra by employing quantum chemical methods. The computational method is outlined in the following.

Computational method

Linear combination of atomic orbitals–molecular orbital–self-consistent-field (SCF) restricted Hartree–Fock (HF) calculations were performed on the different conformers in keto and nitrosophenol forms of lawsoneoxime and its C_3 derivatives as shown in Fig. 1, using the Gaussian 94 program [15] with the internally stored Dunning–Huzinaga [16] full double-zeta basis set. The polarization functions were added on all the atoms. Stationary-point geometries with respect to the nuclear coordinates were derived by the simultaneous relaxation of all the geometric parameters using the analytical gradient method [17]. These geometries were subjected to subsequent optimization, using the hybrid density functional method incorporating Becke's three-parameter exchange–correlation functional (B3LYP) given by Lee, Yang and Parr [18, 19].

The molecular electrostatic potential (MESP), $V(\mathbf{r})$, at a point $\mathbf{r}$ due to a molecular system with nuclear charges $\{Z_A\}$ located at $\{R_A\}$ and the electron density $\rho(\mathbf{r})$ is given by

---

Correspondence to: S. P. Gejji
e-mail: spgejji@chem.unipune.ernet.in

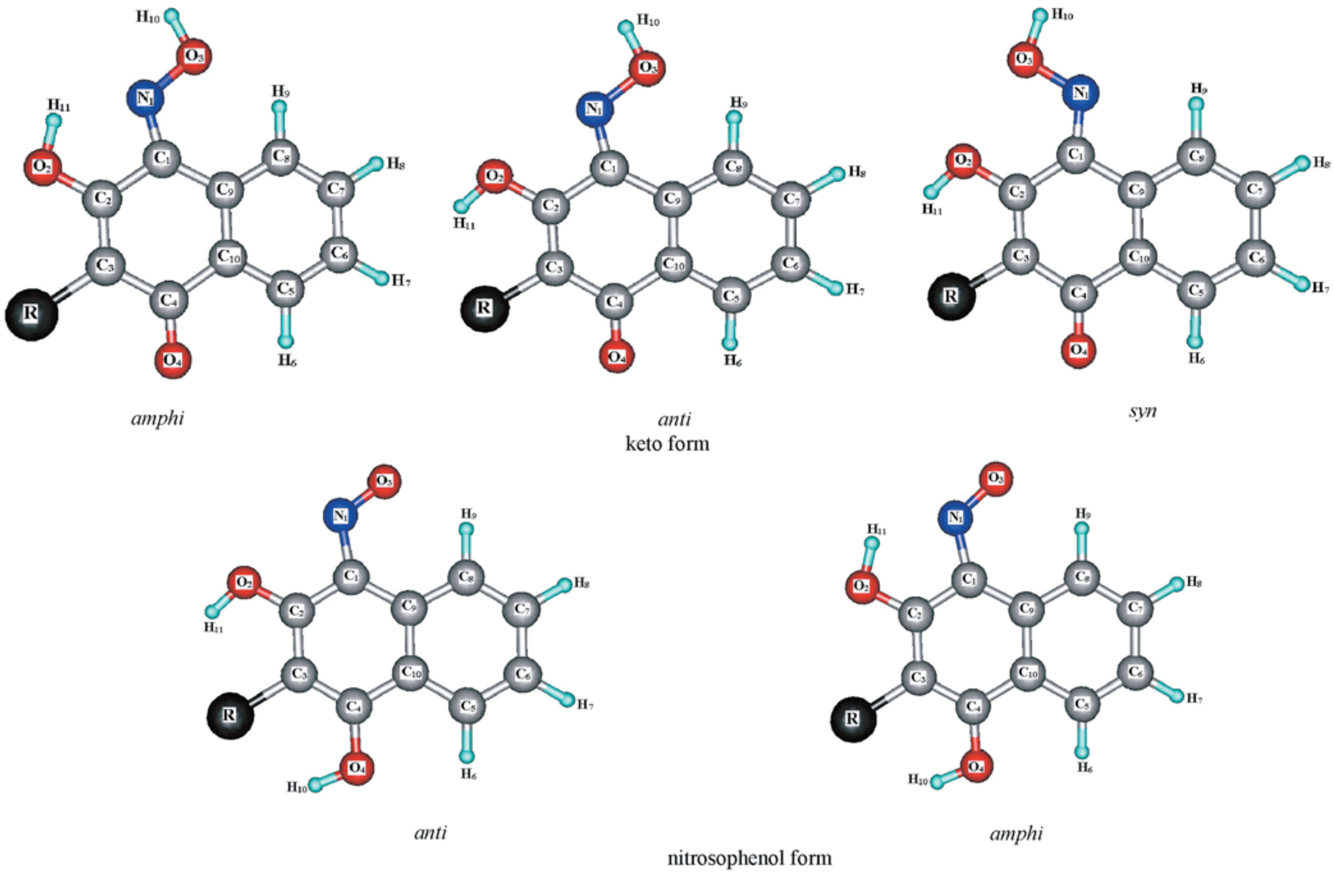

Fig. 1. Keto and nitrosophenol forms of lawsoneoxime and its C_3 derivatives with R as substituent

$$V(\mathbf{r})=\sum_{A=1}^{N}\frac{Z_A}{|\mathbf{r}-R_A|}-\int\frac{\rho(\mathbf{r}')\mathrm{d}^3\mathbf{r}'}{|\mathbf{r}-\mathbf{r}'|}\,, \tag{1}$$

with N being the total number of nuclei in the molecule. Thus Eq. (1) comprises two terms representing the bare nuclear potential and the electronic contributions. The topography of the MESP is mapped by examining the eigenvalues of the Hessian matrix at the point where the gradient $V(\mathbf{r})$ becomes zero. The critical points (CPs) in the MESP were located using the code UNIPROP [20, 21]. For visualization of the MESP topography the UNIVIS-2000 [20, 21] software was used. The MESP CPs can thus be characterized [22, 23] in terms of its rank and signature and further can be grouped into three sets (3, +3), (3, +1) and (3, −1). The (3, +3) set corresponds to the set of minima and the remaining ones turn out to be the saddle points. Thus the location of these CPs and their respective MESP value provide insight into the cation binding. Harmonic vibrational frequencies were calculated from the diagonalization of the force constant matrix. Normal vibrations were assigned by visualizing the displacement of atoms around their equilibrium positions by using the program code UNIVIS-2000.

Results and discussion

Five different conformers of lawsoneoxime and its derivatives ($R=CH_3$, NH_2, Cl, NO_2) considered are displayed in Fig. 1 along with the atomic labels used. The zero-point-energy-corrected relative stabilization energies of the syn, anti and amphi conformers in the keto form as well as for the amphi and anti conformers in the nitrosophenol form are given in Table 1. The uncorrected values are given in parentheses. The zero energies for the C_3 substituent with $R=H$, CH_3, NH_2 and Cl refer to −665.763572, −705.089669, −721.137876 and −1125.346457 au, respectively, and their zero-point-energy-corrected counterparts correspond to −665.609217, −704.907476, −720.966454 and −1125.201437 au. It should be remarked here that for

Table 1. Zero-point-energy-corrected relative stabilization energies (kJ mol^{-1}) for the different conformers of laws oneoxime derivatives. Uncorrected values are given in *parentheses*

R	Keto			Nitrosophenol	
	Amphi	Anti	Syn	Anti	Amphi
H	0.00 (0.00)	24.45 (25.12)	30.14 (30.67)	66.63 (70.86)	20.22 (21.30)
Cl	0.00 (0.00)	10.19 (10.80)	14.59 (15.85)	47.90 (52.20)	12.17 (13.25)
CH_3	0.00 (0.00)	23.54 (26.75)	41.08 (35.53)	78.40 (26.75)	24.25 (25.75)
NH_2	0.00 (0.00)	23.95 (23.27)	26.91 (27.16)	74.60 (78.09)	40.07 (42.63)
NO_2	16.63 (15.75)	0.00 (0.16)	7.41 (8.51)	6.27 (7.35)	0.21 (0.00)

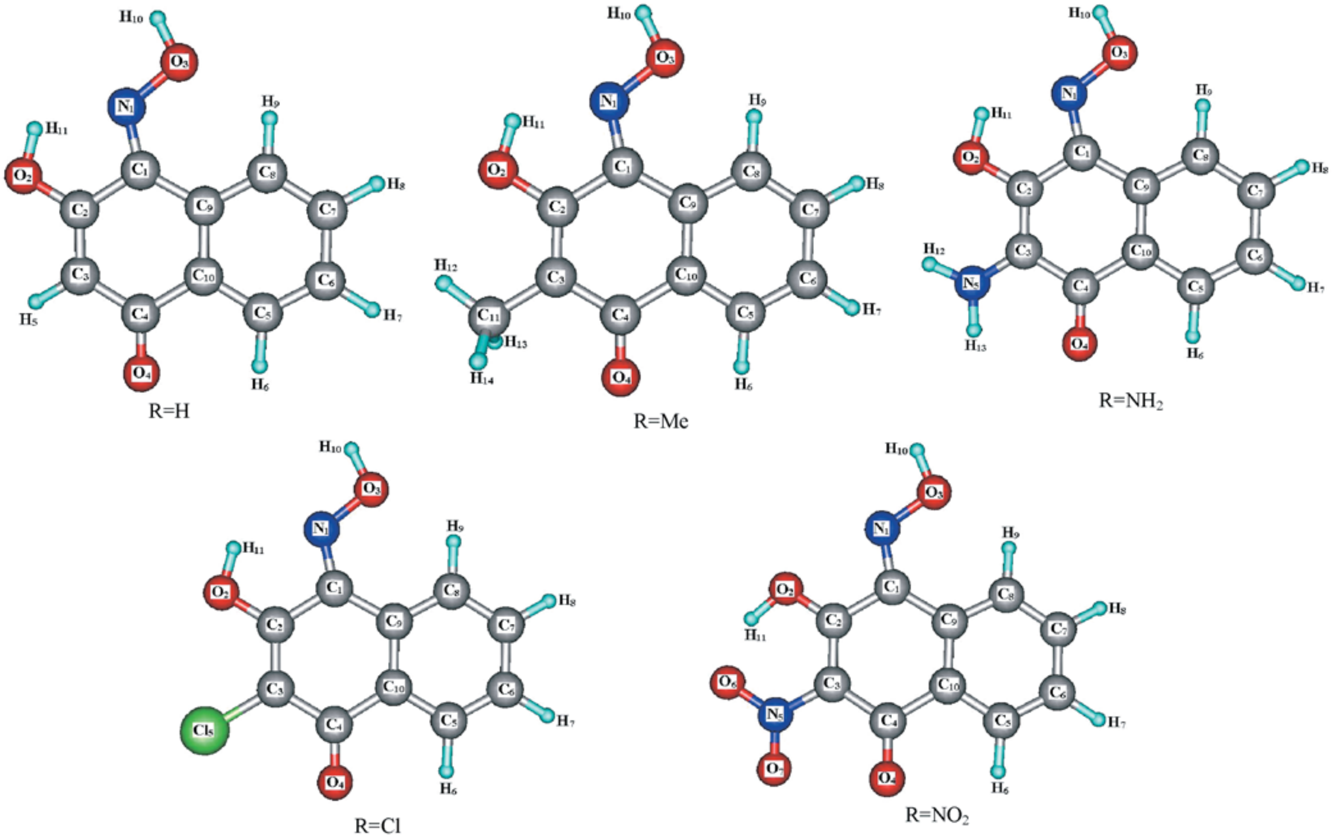

R=H

R=Me

R=NH$_2$

R=Cl

R=NO$_2$

Fig. 2. Lowest-energy conformers of lawsoneoxime and its C_3 derivatives

the nitro derivative the zero-point-energy correction brings about alteration in the rank order of stabilization energies, making the anti conformer (keto form), with its SCF energy of −870.300768 au (correction owing to zero-point energy reduces this to –870.144844 au), to be the stablest. For lawsoneoxime and its derivatives except for nitrolawsoneoxime, the amphi conformer turns out to be the lowest-energy conformer, which is partly attributed to the five-membered-ring formation via the oximino nitrogen and the C_2 hydroxyl proton. In contrast, in the case of nitrolawsoneoxime, such an amphi conformer is predicted to be more destabilized owing to greater electronic repulsions from the nitro group which is nearly perpendicular to the molecular plane. For nitrolawsoneoxime the anti conformer in the keto form and the amphi conformer in nitrosophenol form, both facilitating O–H$\cdots$O hydrogen-bonded interactions, are more stabilized than the other conformers. These hydrogen-bonded interactions via the C_2 or the C_4 hydroxyl proton lead to six-membered-ring formation in the anti and amphi conformers (Fig. 2). The latter is predicted to be only 0.21 kJ mol^{-1} higher in energy than the lowest-energy conformer.

Selected bond distances and bond angles of the lowest-energy conformer of lawsoneoxime and its CH_3-, NH_2- and Cl-substituted derivatives are compared in Table 2. As may be noticed readily the C_3 substitution

Table 2. B3LYP optimized geometrical parameters (bondlengths in angstroms and bond angles in degrees) for lawsoneoxime and its C_3-substituted derivatives

	H	CH_3	NH_2	Cl	NO_2
$r\ (C_1C_2)$	1.493	1.491	1.468	1.490	1.492
$r\ (C_2C_3)$	1.358	1.363	1.368	1.364	1.397
$r\ (C_3C_4)$	1.458	1.468	1.470	1.472	1.482
$r\ (C_4C_{10})$	1.506	1.504	1.495	1.505	1.501
$r\ (C_9C_{10})$	1.419	1.417	1.402	1.418	1.417
$r\ (C_1C_9)$	1.478	1.476	1.483	1.476	1.478
$r\ (C_8C_9)$	1.412	1.412	1.409	1.412	1.413
$r\ (C_7C_8)$	1.399	1.399	1.401	1.399	1.398
$r\ (C_6C_7)$	1.402	1.402	1.400	1.402	1.402
$r\ (C_5C_6)$	1.398	1.398	1.398	1.398	1.396
$r\ (C_5C_{10})$	1.400	1.400	1.400	1.401	1.402
$r\ (C_1N_1)$	1.302	1.303	1.308	1.303	1.304
$r\ (N_1O_3)$	1.382	1.384	1.389	1.381	1.374
$r\ (C_2O_2)$	1.348	1.354	1.363	1.343	1.310
$r\ (C_4O_4)$	1.234	1.235	1.237	1.229	1.225
$r\ (O_2H)$	0.979	0.979	0.977	0.979	1.021
$r\ (O_3H)$	0.970	0.970	0.969	0.970	0.970
$r\ (C_3X)^a$	1.086	1.504	1.382	1.737	1.444
$(C_{10}C_4O_4)$	120.8	120.4	122.0	121.1	120.8
$(C_3C_4O_4)$	122.0	121.2	120.1	122.3	123.8
$(C_1C_2O_2)$	116.9	116.1	118.0	117.1	116.3
$(C_3C_2O_2)$	120.9	120.7	118.8	121.3	123.2
$(C_2C_1N_1)$	110.1	110.2	110.5	109.7	110.6
$(C_9C_1N_1)$	131.2	130.8	130.6	131.0	130.4
$(C_1N_1O_3)$	116.9	116.9	116.7	116.9	115.4
(C_2O_2H)	106.2	105.9	105.7	105.9	104.4
(N_1O_3H)	102.8	102.7	102.5	102.8	102.4
$(C_2C_3X)^a$	120.4	117.9	116.8	117.8	119.5
$(C_4C_3X)^a$	118.1	122.7	123.3	120.3	118.7

[a] *X* is the directly bonded atom from the substituent group

Table 3. Net atomic charges from the electrostatic potential for lawsoneoxime and its C_3-substituted derivatives

	H	Me	NH_2	Cl	NO_2
C_1	0.342	0.386	0.344	0.310	0.381
C_2	0.252	0.055	−0.028	0.239	0.419
C_3	−0.445	−0.156	0.133	−0.194	−0.525
C_4	0.638	0.534	0.551	0.652	0.646
C_5	−0.074	−0.065	−0.015	−0.022	−0.052
C_6	−0.095	−0.076	−0.109	−0.109	−0.090
C_7	−0.143	−0.174	−0.149	−0.154	−0.108
C_8	−0.029	−0.031	−0.038	−0.032	−0.103
C_9	−0.009	−0.042	0.019	0.029	−0.011
C_{10}	−0.114	−0.096	−0.176	−0.198	−0.149
N_1	−0.286	−0.269	−0.261	−0.277	−0.245
O_2	−0.511	−0.435	−0.432	−0.497	−0.695
O_3	−0.416	−0.439	−0.451	−0.409	−0.432
O_4	−0.567	−0.524	−0.517	−0.538	−0.507
X^a		−0.082	−0.789	−0.075	0.948
O_6					−0.627
O_7					−0.426

[a] X is the directly bonded atom from the substituent group

results in an increase of 0.006–0.015 Å in the C_2O_2 bond distances, partly attributed to the inductive effect of the substituent. Generally, the bond angles deviate within 1°. The bond distances and the bond angles of nitrolawsoneoxime in its anti conformer are also presented in Table 2.

The net atomic charges of the lowest-energy conformers of lawsoneoxime and its derivatives obtained from the molecular electrostatic potential, calculated using the HF wavefunction, are reported in Table 3. As may readily be noticed the carbonyl oxygen atom (O_4) turns out to be most electron rich in lawsoneoxime and its methyl- or chloro-substituted derivatives as well. For aminolawsoneoxime, however, the amino nitrogen (N_5) center retains more residual electronic charge than any of the oxygens. It may further be remarked here that in nitrolawsoneoxime, which refers to the anti conformer, the larger electronic charge resides on the O_2 atom, partly attributed to the intramolecular $O{-}H\cdots O$ hydrogen bonding. The MESP isosurface of $V = -157.5$ kJ mol^{-1} is depicted in Fig. 3. Thus it may be inferred that the three-dimensional network of these crystals extends through the $C{=}O\cdots H$ intermolecular hydrogen-bonded interactions. These intermolecular bonds (1.87 Å) are observed in the single-crystal X-ray data of the methyl-substituted derivative. The (3, +3) MESP CPs near oxygen and nitrogen atoms are presented in Table 4 along with their respective MESP values. Thus the MESP values at the deepest minima for the carbonyl oxygen follow a trend, $CH_3 > NH_2 > Cl$, which can be explained on the basis of the inductive effect of the C_3 substituent. It should be noted here that the deepest minimum near the N_1 atom turns out to be positive only for chlorolawsoneoxime and is partly attributed to the combined result of the electron-withdrawing nature of the chloro substituent and the $N\cdots H$ hydrogen-bonding interactions which results in the depletion of electron density from the oximino nitrogen. The hydrogen bonding from the oximino nitrogen is not present in the nitrolawsoneoxime conformer.

The B3LYP vibrational frequencies of the lowest-energy conformers are given in Table 5. As may be noted the $C{=}O$ stretching shows an upshift of 9 cm^{-1} in the chloro derivative, which increases further by 18 cm^{-1} for the nitro compound relative to the corresponding vibration in lawsoneoxime ($R{=}H$), whereas for methyllawsoneoximes and aminolawsoneoximes a downshift of 14 cm^{-1} is predicted. The trend for the N_1O_3 stretching in the different C_3-substituted derivatives of lawsoneoxime is in accordance with the bond lengths displayed in Table 2. Further, in the anti conformer of nitrolawsoneoxime the strong $O_2\cdots H$ intramolecular hydrogen bond results in a large downshift for the OH stretching. Consequently the phenolic O_2H and C_1N_1 (from the oxime) stretching vibrations are very intense owing to larger charge separation of the respective atoms compared to the corresponding stretchings in other derivatives. Further a downshift of 15–29 cm^{-1} for the C_2O_2 stretching vibration relative to that in lawsoneoxime is predicted for amphi conformers where the intramolecular hydrogen bonds with the oximino nitrogen are present. A shift in the opposite direction is predicted for the nitro derivative. Thus the $O{-}H\cdots O$ hydrogen-bonded interactions in nitrolawsoneoxime influence the conformational energetics and the vibrational frequencies.

Conclusions

The optimized structures of lawsoneoxime and its C_3-substituted derivatives ($R{=}CH_3$, NH_2, Cl, NO_2) have been obtained. Except for the nitro derivative all other C_3-substituted derivatives engender the amphi conformer in the keto form as the lowest minimum, which may partly be attributed to the five-membered-ring formation through hydrogen-bonded interactions (the $N\cdots H$ bond distance ranging from 1.919 Å for $R{=}CH_3$ to 1.971 Å for $R{=}NH_2$). The nitro derivative, however, shows the anti conformer (keto form) to be the lowest-energy conformer, which is only 0.21 kJ mol^{-1} stabler than the amphi conformer in the nitrosophenol form. Both these conformers have intramolecular hydrogen bonds (1.504 and 1.522 Å, respectively) facilitated through β-hydroxyl and α-hydroxyl groups, which results in a six-membered ring. The CN and NO bond distances of the oxime group in these derivatives are nearly insensitive to the C_3 substitution of lawsoneoxime. The charge distribution studies based on the MESP support the presence of $C{=}O\cdots H$ intermolecular hydrogen bonds in an extended three-dimensional network. Assignments of normal vibrations reveal that the frequencies of the $C{=}O$ stretching vibrations in lawsoneoxime are upshifted for the electron-withdrawing substituents ($R{=}Cl$, NO_2), whereas a shift in the opposite direction (downshift of nearly 14 cm^{-1}) is predicted for the CH_3 and NH_2 derivatives. Thus in brief, intramolecular hydrogen bonding is important in

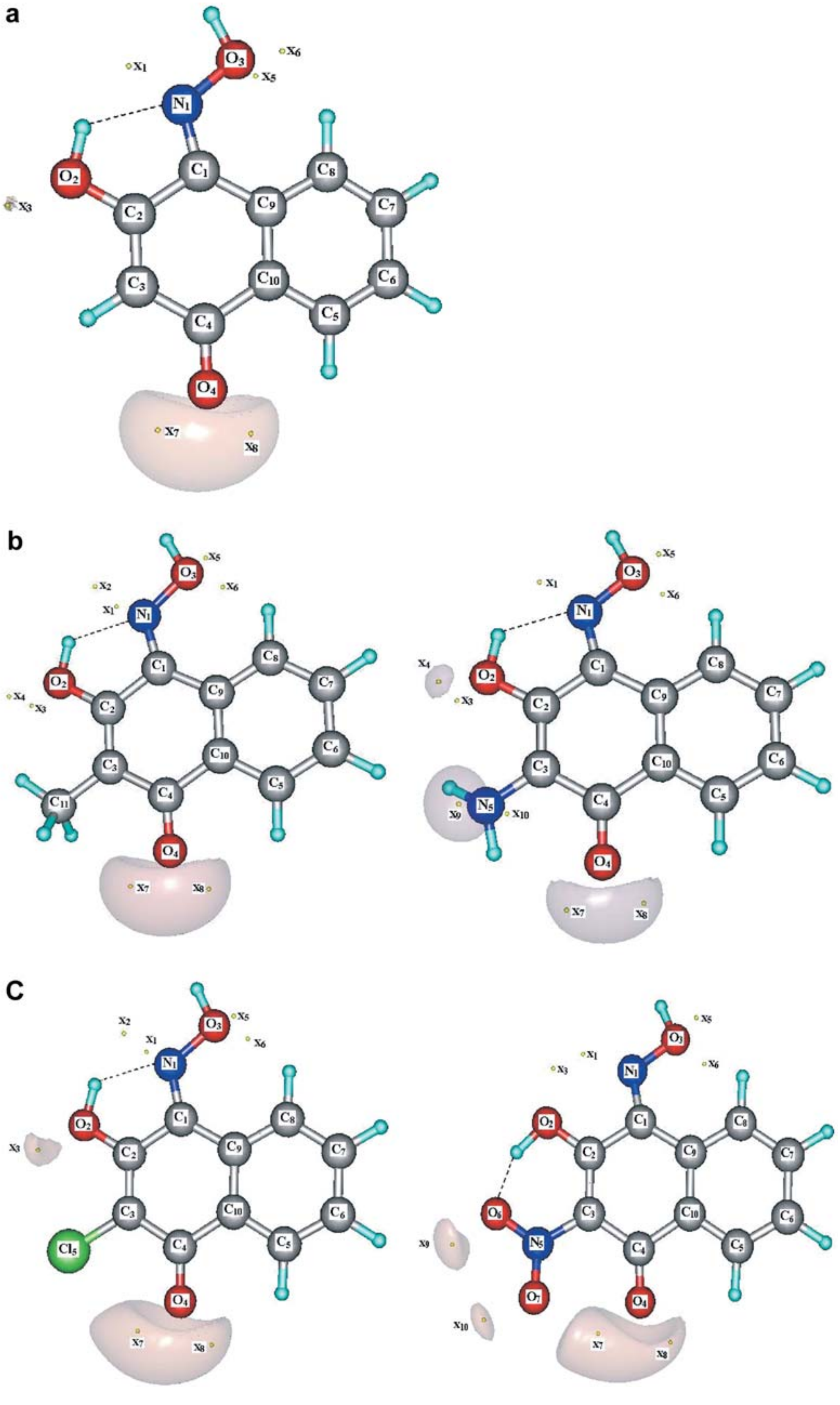

Fig. 3. Molecular electrostatic potential isosurface ($V = -157.5$ kJ mol^{-1}) and (3, +3) minima for **a** lawsoneoxime, **b** methyllawsoneoxime and aminolawsoneoxime, and **c** chlorolawsoneoxime and nitrolawsoneoxime

Table 4. The molecular electrostatic potential minima(kJ mol^{-1}) for different lawsoneoxime derivatives

Atom		H	CH_3	NH_2	Cl	NO_2
N_1	x_1	−0.7	−25.1	−47.0	16.0	−147.3
	x_2				16.5	
O_2	x_3	−160.9	−158.2	−175.8	−173.7	−147.3
	x_4		−158.2	−154.0		−12.9
O_3	x_5	−76.7	−80.8	−106.3	−62.5	−28.9
	x_6	−76.7	−85.8	−102.4	−62.4	−62.1
O_4	x_7	−262.7	−248.2	−209.0	−205.5	−258.8
	x_8	−227.7	−219.8	−196.5	−202.0	−189.5

Table 5. B3LYP frequencies for selected normal vibrations (cm^{-1}) for lawsoneoxime and its C_3-substituted derivatives

	H	CH_3	NH_2	Cl	NO_2
O_3H stretch	3,820 (178)	3,821 (173)	3,827 (174)	3,818 (187)	3,809 (206)
O_2H stretch	3,651 (113)	3,643 (122)	3,672 (99)	3,638 (122)	2,853 (481)
C_4O_4 stretch	1,721 (319)	1,706 (253)	1,707 (268)	1,730 (193)	1,748 (246)
C_1N_1 stretch	1,652 (11)	1,653 (8)	1,636 (30)	1,649 (22)	1,655 (192)
C_2O_2 stretch	1,443 (291)	1,428 (212)	1,425 (35)	1,414 (277)	1,489 (264)
N_1O_3 stretch	1,061 (160)	1,070 (83)	1,047 (127)	1,069 (109)	1,122 (105)

predicting the energy rank order, charge distribution and the vibrational spectra of different conformers of lawsoneoxime derivatives.

Acknowledgements. S.P.G. is grateful to the Council of Scientific and Industrial Research (CSIR, project 01(1772)/02/EMR-II), New Delhi, India. K.A.J. thanks the CSIR for a Junior research fellowship. D.R.T. acknowledges support through the UGC minor research project.

References

1. Bermejo MR, Gonzalez AM, Fondo M, Deibe AG, Maneiro M, Sanmartin J, Hoyos OL, Watkinson M (2000) New J Chem 24: 235
2. Pierpont CG, Lange CW (1994) Prog Inorg Chem 41:331
3. Pierpont CG, Buchanan RM (1981) Coord Chem Rev 38:45
4. Anderson BA, Styring S (1991) In: Lee CP (ed) Photosystem-II: molecular organization, function of acclimation, vol 16. Academic, San Diego, p 1
5. Diner BA, Babcock GT (1996) In: Ort D, Yocum C (eds) Oxygenic photosynthesis: the light reactions. Kluwer, Dordrecht, p 213
6. Debus RJ (1992) Biochim Biophys Acta 1102:269–352
7. Barber J, Anderson B (1994) Nature 370:31
8. Rutherford AW, Zimmerman JL, Boussac A (1992) In: Barber J (ed) The photosystems. Structure, function and molecular biology. Elsevier, Amsterdam, p 179
9. Bour JJ, Steggergada JJ (1967) Chem Comm 85
10. Bhattacharya S, Mukherjee RN, Chakravorty A (1986) Inorg Chem 25:3448
11. Steggergada JJ, Bour JJ (1970) Proc Symp Coord Chem 174
12. Ammon HL, Bhatacharjee SK, Henry-Logan KR (1983) Acta Crystallogr Sect C 39:355
13. Rane SY, Dhavale DD, Mulay MP, Khan EM (1990) Spectrochim Acta Part A 46: 113
14. Thube DR, Todkary AV, Joshi KA, Rane SY, Gejji SP, Salunke SA, Marrot J, Varret F (2002) J Mol Struct (THEOCHEM) 622: 211
15. Frisch MJ, Trucks GW, Schlegl HB, Gill PMW, Johnson BG, Robb MA, Cheeseman JR, Keith T, Petersson GA, Montgomery JA, Raghavachari K, Al-Laham MA, Zakrzewski VG, Ortiz JV, Foresman JB, Ciosloski J, Stefanov BB, Nanayakkara A, Challacombe M, Peng CY, Ayala PY, Chen W, Wong MW, Andres JL, Replogle ES, Gomperts R, Martin RL, Fox DJ, Binkley JS, Defrees DJ, Baker J, Stewart JP, Head-Gordon M, Gonzalez C, Pople JA (1995) Gaussian 94. Gaussian, Pittsburgh, PA
16. Dunning Jr, Hay PJ (1976) In: Schaefer HF III (ed) Modern theoretical chemistry. Plenum, New York, p 1
17. Pulay P (1969) Mol Phys 17: 197
18. Becke AD (1993) J Chem Phys 98: 5684
19. Lee C, Yang W, Parr RG (1988) Phys Rev B 37: 785
20. Limaye AC, Gadre SR (2001) Curr Sci India 80:1298
21. Gadre SR, Shirsat RN (2000) Electrostatics of atoms and molecules. Universities Press, Hyderabad, India
22. Gadre SR, Shrivastava IH (1991) J Chem Phys 94: 4384
23. Gadre SR, Kulkarni SA, Shrivastava IH (1992) J Chem Phys 96: 5253